HHS Public Access

Author manuscript

Neurobiol Aging. Author manuscript; available in PMC 2019 July 01.

Published in final edited form as:

Neurobiol Aging. 2018 July ; 67: 108–119. doi:10.1016/j.neurobiolaging.2018.03.015.

Age-related defects in short-term plasticity are reversed by acetyl-L-carnitine at the mouse calyx of Held

Mahendra Singh[a], **Pedro Miura**[b], and **Robert Renden**[a,#]

[a]Department of Physiology and Cell Biology, University of Nevada, Reno School of Medicine, Reno, NV 89557, USA

[b]Department of Biology, University of Nevada, Reno, Reno, NV 89557, USA

Abstract

Hearing acuity and sound localization are affected by aging and may contribute to cognitive dementias. While loss of sensorineural conduction is well documented to occur with age, little is known regarding short-term synaptic plasticity in central auditory nuclei. Age-related changes in synaptic transmission properties were evaluated at the mouse calyx of Held, a sign-inverting relay synapse in the circuit for sound localization, in juvenile adults (one month old) and late-middle age (18–21 months old) mice. Synaptic timing and short-term plasticity were severely disrupted in older mice. Surprisingly, acetyl-l-carnitine (ALCAR), an antinflammatory agent that facilitates mitochondrial function, fully reversed synaptic transmission delays in aged mice to reflect transmission similar to that seen in juvenile adults. These findings support ALCAR supplementation as an adjuvant to improve short term plasticity and potentially CNS performance in animals compromised by age and/or neurodegenerative disease.

Keywords

neurotransmission; acetyl-l-carnitine; calyx of Held; aging; synaptic plasticity; electrophysiology

[#]Corresponding Author: 1664 N. Virginia St., Reno NV 89557. rendenr@unr.edu.

Declaration of conflicts of interest: none.

Author Contributions: Designed and executed experiments: MS, PM, RR. Data analysis: MS, RR. Edited and revised manuscript: MS, PM, RR. All authors have approved the final article.

All Authors Disclose:

1. Authors declare no conflict of interest.
2. All sources for financial support are outlined in teh acknowledgements section of the Manuscript.
3. All data and work included in this study are original research, and have not been published previously, or submitted for publication elsewhere.
4. Appropriate approval and procedures were used with regards to vertebrate animal subjects used in this study, and approved by our institutional committee on Animal care and use, as outlined in the Methods section of the manuscript.

1. Introduction

Age-related hearing loss in both humans (presbycusis) and rodent models is often attributed to a mixed loss of peripheral sensory neurons (inner and outer hair cells), and/or spiral ganglion cells, resulting in sensorineural deafness (Gates and Mills, 2005). While loss of these peripheral neurons results in hearing degradation at the earliest synaptic relays, less information is available on age-related changes in central synapses of the auditory system. Hearing loss induced by noise or ototoxic drug treatment is followed within weeks by significant plasticity within the auditory system from brainstem to cortical regions, to compensate for loss of frequency-specific input (Eggermont, 2017; Wolak et al., 2017). Central auditory processing defects associated with presbycusis have been observed (Humes et al., 2012); however, functional changes in central synaptic transmission, including changes in short-term plasticity, have not been adequately evaluated in age-related hearing loss models.

Computation for spatial localization of sound in the horizontal plane occurs via the superior olivary complex (SOC) in the auditory brainstem. These binaural circuits are specialized for detecting submillisecond differences in interaural timing and single decibel differences in sound level (reviewed in (Grothe et al., 2010). As such, even minor alterations to timing and synaptic function may result in degraded hearing, especially in complex auditory environments (e.g. the ‘cocktail party problem’) where speech segregation is enhanced by spatial sound localization (Hawley et al., 2004). In one of the binaural auditory brainstem circuits used for sound localization, globular bushy cells of the ventral cochlear nucleus project axons contralaterally, terminating in monosynaptic excitatory inputs onto principal neurons in the medial nucleus of the trapezoid body (MNTB) (Cant and Benson, 2003; Harrison and Warr, 1962). In the MNTB, the calyx of Held synapse acts as a reliable sign-inverting relay, with the ability to fire at near kHz frequency with exquisite temporal precision (reviewed in (Borst and Soria van Hoeve, 2012).

The calyx of Held, a giant glutamatergic synapse specialized for high frequency transmission, has been exploited as a model synapse for understanding chemical neurotransmission, and has a specialized role in maintaining synaptic fidelity and timing (reviewed in (Wichmann, 2015). Of particular experimental advantage, calyx of Held synapses generally terminate in a giant unitary axosomatic innervation onto a given principal cell body, easing interpretation of electrophysiology data. This synapse has been studied extensively in neonatal rodents prior to hearing and during maturation following hearing onset, up to about 20 days after birth. However, very little information on the details of this synapse exist in the adult, and no recordings have been performed previously at this synapse to evaluate age-related changes in transmission fidelity towards the end of the natural life span. Previous work has revealed age-related transmission defects in central auditory synapses at the endbulb of Held, in the ventral cochlear nucleus (Xie, 2016; Xie and Manis, 2017; 2013). Notably, the postsynaptic bushy cells at this synapse give rise to projections that terminate in the presynaptic calyx of Held. It is unknown if similar defects as those described at the endbulb of Held are present in other central nuclei in the sound localization circuit, e.g. at the calyx of Held in auditory brainstem.

Causes for age-related hearing loss vary, with a contribution of both genetic and environmental factors. The C57BL/6J inbred mouse strain is widely used for aging research and displays typical age-related hearing loss by 12–15 months of age (Hunter and Willott, 1987; Keithley et al., 2004). Significant age-related loss of sensitivity to sounds embedded in noise is observed in recordings from the VCN of these mice as early as six months after birth (Willott et al., 1991). Mitochondrial dysfunction and increased oxidative stress have emerged as a common theme both for age-related cognitive decline and hearing loss (Han and Someya, 2013; Lin and Beal, 2006; Someya and Prolla, 2010). Therefore, treatment with facilitators of mitochondrial metabolism, which also act to suppress tissue oxidation, have been employed as a potential therapy for age- and disease-related loss of neuronal function (L. Chen et al., 2014; Hagen et al., 2002; Mehrotra et al., 2015). For example, feeding aged mice acetyl-l-carnitine (ALCAR), which facilitates mitochondrial function and suppresses formation of antioxidants, acts to reverse defects in behavioral outcomes like disease-related memory loss (Barnes et al., 1990; Huang et al., 2010; Liu et al., 2002). Hearing has also been shown to improve with ALCAR treatment (S. H. Choi and C.-H. Choi, 2015; Coleman et al., 2007; Kopke et al., 2005).

In this study, we investigated synaptic transmission changes between juvenile and aged mice in the auditory brainstem, focusing on the effects of age on short-term plasticity at the calyx of Held synapse, a central relay in the auditory brainstem circuit for sound localization. From recordings of transmission at the calyx of Held we observed increased synaptic depression and altered short-term synaptic plasticity in older versus young mice. In an attempt to ameliorate age-induced loss of short term synaptic plasticity, we orally administered ALCAR for one month and found that it reversed transmission defects at the calyx of Held synapse in the older mice. These results support the concept that facilitators of mitochondrial metabolism and antioxidants may be an extremely effective therapy to increase synaptic function and restore short-term plasticity in aged brains, and provide for the first time a clear mechanism of action for ALCAR on activity-dependent synaptic transmission.

2. Experimental Procedures

2.1 Animals

Inbred mice from C57BL/6J genetic background of both sex were used at 1 month old. Male mice of 18–21 months old and the same genetic background were obtained from NIA Division of Aging Biology Aged Rodent Colony. Mice were group housed at 3–5 animals per cage. All animal protocols and experiments were approved by the Animal Care and Use Committee at University of Nevada, Reno.

2.2 Immunohistochemistry

Mice were deeply anesthetized, and brains fixed *in vivo* by cardiac perfusion with 4% paraformaldehyde in 0.1 M phosphate buffered saline (PBS). Brains were removed, and postfixed overnight at 4°C in 4% paraformaldehyde-PBS. Brain slices ~60 um thick were made using a tissue slicer (OTS 4500; EMS, Hatfield PA). Generally, 8–10 sections were retrieved per animal. Free-floating slices containing the MNTB were permeabilized with

0.5% Triton-X 100 and blocked with 3% fish gelatin and 0.025% sodium azide, in PBS at RT for 30 min, with mild agitation on a nutator. Slices were stained overnight at 4°C with mouse anti-MAP2 (1:1000, Millipore-Sigma MAB3418) and guinea pig anti-vGluT1(1:5000, Synaptic Systems) in PBS with gentle agitation. Alexa 488- and Alexa 647-conjugated secondary antibodies (ThermoFisher Scientific) were used at 1:1000 and incubated overnight at 4°C in PBS. Residual background tissue fluorescence was quenched with 100 mM glycine in PBS prior to mounting and imaging.

2.3 Confocal Microscopy

Slices were mounted in SlowFade™ Gold (ThermoFisher Scientific) and visualized at 200× on an Olympus Fluoview 1000 laser scanning microscope. Images containing the MNTB were acquired at diffraction-limited lateral resolution, in 9–15 μm thick stacks, bilaterally. Images were analyzed semi-autonomously using algorithms in Volocity 6.30 (Perkin Elmer). Briefly, a region of interest (ROI) encompassing the MNTB was drawn manually, based on vGluT1 signal in the calyx of Held terminal, and appearance of MAP2-positive postsynaptic cell soma. Individual cells were identified using threshold-based detection of MAP2 signal, and mean size of objects per MNTB profile was reported. Density of cells within the MNTB was calculated as the ratio of the sum of somatic objects over the volume of the MNTB ROI.

2.4 ALCAR Supplementation

Male mice at 18–21 months old were housed at 3–4 animals per cage, and given a solution of 1.5% wt./vol O-Acetyl-l-carnitine hydrochloride (ALCAR; Millipore-Sigma #A6706) in drinking water, pH adjusted to ~6 with NaOH, and allowed to drink *ad libitum* for one month prior to recordings, following previously published protocols (Hagen et al., 2002). ALCAR solution was protected from light and exchanged every 3–4 days. Control mice at the same age were given water at ~pH 6. By measuring change in bottle weight, we calculated that ALCAR-treated mice ingested a daily dose of ~2.9 g/kg/day, for one month prior to experimentation. Animals were supervised daily by the UNR Office of Animal Resources, and no adverse effects were reported.

2.5 Electrophysiology

Acute brainstem slices containing the MNTB were prepared as previously described (Lujan et al., 2016; Mahfooz et al., 2016). Briefly, animals were deeply anesthetized with isofluorane, and decapitated. The brain was rapidly removed and immersed in room temperature oxygenated slicing buffer with the following composition (in mM): 85 NaCl, 2.5 KCl, 25 glucose, 25 $NaHCO_3$, 1.25 NaH_2PO_4, 75 sucrose, 0.5 $CaCl_2$, 7 $MgCl_2$, 3 myo-inositol, 2 Na-pyruvate, 0.4 ascorbic acid; pH 7.3 when bubbled with carbogen gas (95% O_2-5% CO_2). Transverse brain stem slices containing the MNTB were made at a thickness of 200 μm using a vibratome (VT 1200S, Leica Microsystems, Oberkochen Germany). Slices were transferred to an incubation chamber containing recording artificial cerebrospinal fluid (ACSF) with the following composition (in mM): 125 NaCl, 2.5 KCl, 25 glucose, 25 $NaHCO_3$, 1.25 NaH_2PO_4, 2 $CaCl_2$, 1 $MgCl_2$, 3 myo-inositol, 2 Na-pyruvate, 0.4 ascorbic acid, and bubbled with carbogen gas for 30–60 minutes at 35°C and maintained thereafter (up to 6 hours) at room temperature (~23°C) until used for recording.

Slices were perfused at ~2 mL/min with normal ACSF solution bubbled with carbogen gas in a recording chamber and visualized using gradient contrast optics with a 63× (1.0 NA) Apochromat objective on Zeiss AxioExaminer.A1 microscope. Recordings were performed at room temperature (23–25°C). Glass electrodes (1.5 mm OD; WPI Inc., Sarasota FL) were pulled to open tip resistance of 1.5–3 MΩ on a Sutter P1000 puller (Novato CA) and contained (in mM): 130 Cs-gluconate, 10 CsCl, 5 Na_2-phosphocreatine, 10 HEPES, 5 EGTA, 10 TEA-Cl, 4 Mg-ATP, 0.5 GTP, 5 QX-314 adjusted to pH of 7.2 with CsOH. Density of internal solution was 310–315 mOsm. Principal cell neurons in the MNTB were voltage-clamped using an Axon MultiClamp 700B amplifier controlled by MultiClamp Commander software (Molecular Devices, Sunnyvale CA). Data were low-pass filtered at 2.9 kHz and digitized at sampling rates of 10 kHz. Electrophysiology data were analyzed offline using custom-written routines in IGOR Pro (Wavemetrics, Lake Oswego OR). Series resistances (R_S) for voltage clamped cells ranged from 2–8 MΩ and was routinely compensated to <0.5 MΩ for the duration of the recording. Cells were routinely held at −70 mV command voltage, but not corrected for liquid junction potential, estimated to be −11 mV based on solution composition. Excitatory postsynaptic currents (EPSC) were evoked by placing a bipolar stimulating electrode near the midline and applying a biphasic voltage waveform (100 μs duration, <5 V). All evoked EPSC recordings were induced by applying stimulation ~0.5 V over threshold. AMPA-mediated EPSC recordings were performed in normal ACSF solution, with added 50 μM D-AP5 to block NMDA receptors, 0.5 μM strychnine to inhibit glycine receptors, and 10 μM bicuculline to inhibit $GABA_A$ receptors. Kynurenic acid (1 mM) was included in the bath solution to decrease receptor desensitization (Wong et al., 2003), but was not used for recording of spontaneous (quantal) events.

Maximum curvature method was used to determine the onset of EPSC waveforms, using methods previously published (Fedchyshyn and Wang, 2007). Briefly, a Boltzman charge-voltage equation was used to fit the initial onset of the EPSC, in the form

$$f(t) = I_{max}/(1 + exp((t_{mid} - t)/t_c)) + C, \quad (1)$$

Where I_{max} is the EPSC amplitude, t_{mid} is the midpoint of the fitting region. Levenberg–Marquardt with least-squares minimization (Clampfit 10.6) was used to obtain best-fit parameters.

Then, the fourth derivative was solved, and set to zero. Evaluations of the equation gave three solutions, where

$$t_1 = t_{mid} - ln(5 + 2\sqrt{6})t_c, \quad (2)$$

$$t_2 = t_{mid} \quad (3)$$

$$t_3 = t_{mid} - ln\,(5 - 2\sqrt{6})t_c, \quad (4)$$

Solutions for eq. 2 and 4 give the time of maximum curvature, and solution that occurred earliest in time was used to for EPSC onset.

Quantal recordings of spontaneous activity were taken from synapses where evoked responses could be recorded, but prior to high frequency stimulation. Spontaneous activity was recorded continuously for ~2 min per cell, and events were detected using a sliding window threshold detection algorithm, for peaks larger than 14 pA from baseline. Median event amplitudes were reported to avoid potential skewing due to rare but large events. Previous studies at this synapse in juvenile mice report quantal events are ~39 pA using similar threshold detection methods (Takami et al., 2017).

Readily releasable pool size was estimated using the method of Wesseling and Lo, as described previously for the calyx of Held (Mahfooz et al., 2016). In brief, the integral of responses during a 300 Hz stimulation were measured after removing stimulus artifacts. RRP size at rest and maximal unitary recruitment rate can be determined numerically by comparing the initial release probability determined by measuring the RRP as a sum of all responses in a high frequency train to the release probability during steady state responses, in cases where the initial RRP is driven toward complete depletion. We refer the reader to the primary publications for more detailed explanation of this method (Mahfooz et al., 2016; Wesseling and Lo, 2002)1.

2.6 Reagents

All salts and pharmacological agents were purchased from Sigma-Aldrich (St. Louis MO), Tocris Biosciences/R&D Systems (Minneapolis MN), and/or Alomone Labs (Jerusalem, Israel) at ≥ 99% or highest purity offered.

2.7 Statistics

Data were analyzed and presented using Prism 7 (Graphpad, La Jolla CA) and Igor Pro 6.37 (Wavemetrics, Lake Oswego OR). Statistical tests used were unpaired Student’s t-test for two groups, and one-way ANOVA with Tukey’s post hoc test, corrected for multiple comparisons when more than two groups were compared. ANOVA p-value and degrees of freedom are reported at the first instance of each test. Biological replicates (N) are reported as individual cells for electrophysiology, and as number of animals (N) and fields of view (n) for immunohistochemistry. Values are reported as mean ± SEM. Significance is reported in figures as *P<0.05, **P<0.01, ***P<0.001, and ****P<0.0001.

3. Results

3.1 Age-related changes in MNTB neuronal density and principal cell size

At 1 month after birth, hearing in mice is developmentally mature, and age-related hearing degeneration has not commenced (Heffner et al., 2001). By 18 months, mice have reached late-middle age. Most slice recording studies have focused on ages <30 days old. MNTB from young juvenile adults (1-month) and older (late-middle age; 18-month old) mice were examined for the presence of principal cell nuclei, and glutamatergic innervation (Figure 1). We marked postsynaptic neuronal cells with MAP2 and the glutamatergic presynaptic terminal with vesicular glutamate transporter 1 (vGLuT1), which primarily labels the calyceal input onto these cells (Dondzillo et al., 2010). The MNTB could be clearly observed in both young and older mice (Fig. 1A). Principal cell size and density were measured bilaterally in 60 um thick slices from three animals at each age. In older mice, principal cell size was significantly reduced compared to 1-month old mice (1058 ± 30.1 um^3 in 18-month old mice, n=43 images, *versus* 1176 ± 30.1 um^3, n=37 images in 1-month old mice, P=0.0442, t=2.055 df=60.94, unpaired t test; Fig. 1B). Principal cell density, taken as the ratio of MAP2 signal within the MNTB, was 0.1308 ± 0.0057 in 1-month old mice, and reduced by 36.2 ± 3.1% in 18-month old mice (P<0.0001, t=6.914 df=78, unpaired t test; Fig. 1C). ROI size for the MNTB was reduced in 18-month old mice (610.5 ± 46.3mm^3) but was not significantly smaller than for 1-month old mice (716.2 ± 34.1 mm^3; P=0.0652, t=1.870, df=78, unpaired t test). The average number of cells in each MNTB profile was also reduced by 15.4% (data not shown), consistent with previous reports of cell loss in C57BL/6 mice at this nucleus (O'Neill et al., 1997), and also for aged rats (Casey and Feldman, 1988). vGluT1-positive signal was present adjacent to all MAP2-positive cells in the MNTB at both 1 month and 18 months (data not shown). While neurons in the MNTB are lost over the course of aging, our results confirm that MNTB neurons are innervated by vGlut1-positive calyx inputs similarly at 1 month and 18 months.

3.2 Age-related changes in synaptic function at the calyx of Held

We next sought to extend our analysis of the aging auditory hindbrain to investigate properties of synaptic transmission. We decided to focus on synaptic transmission at the calyx of Held synapse in the auditory central nervous system in the brain stem of juvenile adult (1-month old) and late middle-age (18 to 21-month old) mice. Much is known about the function of the calyx of Held synapse in young and juvenile rodents, and fidelity and timing of synaptic transmission are critically important functions. However, age-related changes in transmission at this synapse are poorly understood. Aging is known to impair function of the endbulb of Held, a giant synapse formed in the ventral cochlear nucleus, which is also used in for sound localization (Xie, 2016; Xie and Manis, 2017). We hypothesized that age might impact efficacy of synaptic transmission at the calyx of Held. Additionally, dietary supplementation with ALCAR, an anti-inflammatory compound that facilitates mitochondrial function, is known to improve synaptic resilience and plasticity (Kocsis et al., 2016). We hypothesized that facilitated short-term plasticity may be in part responsible for ALCAR in hearing improvement (S. H. Choi and C.-H. Choi, 2015; Coleman et al., 2007; Kopke et al., 2005).

3.2.1 Synaptic delays are severely affected in aging mice—First, we examined the size and timing of EPSCs from principal neurons of MNTB in response to low-frequency stimulation at 0.1 Hz (Figure 2). Compared to 1-month old mice (2.81 ± 0.41 nA, N=11), 18-month old mice showed a significant increase in evoked EPSC amplitude (5.72 ± 0.89 nA, N=12, P=0.0418, Tukey multiple comparison test following one-way ANOVA; F(2,28)=3.273, P=0.0528; Fig. 2B). Treatment of aged mice with the nutritional supplement ALCAR has previously been found to improve hearing and synaptic plasticity in aged mice, but the effect on synaptic function in auditory synapses is unknown. Thus, we sought to undertake a comprehensive electrophysiological characterization of 1-month, 18-month, and 18-month old mice treated with ALCAR (18-month ALCAR). We treated aged mice for 1 month by oral administration of ALCAR and found that evoked EPSC amplitude was slightly reduced by ALCAR, but not significant compared to untreated 18-month old mice (4.21 ± 1.23 nA, N=8; P=0.4575 vs untreated, Tukey multiple comparison test following one-way ANOVA; Fig. 3B).

We noted that 18-month old mice showed a profound defect in the temporal components of synaptic transmission (Fig. 2A). Two discrete components can be seen in most EPSC waveforms that sum to generate transmission delays: conduction delay (CD, time between stimulation peak and pre-AP waveform), synaptic delay (SD, time between pre-AP waveform and onset of the EPSC), and transmission delay (TD, sum of SD and CD; Fig. 2C). The maximum curvature method (described in (Fedchyshyn and Wang, 2007) was used to evaluate the timing of these components. We did not observe any change in the conduction delay in 1-month versus 18-month old mice (1-month: 592.2 ± 23.4 μs, N=9; 18-month: 715.0 ± 60.1 μs, N=6; ALCAR: 603.3 ± 36.6 μs, N=6; P=0.0812, F(2,18)=2.897, One-way ANOVA, fig. 2D). However, we did observe that synaptic delay was significantly increased in old mice relative to juvenile adults (1-month: 295.6 ± 21.9 μs versus 18-month: 421.7 ± 19.4 μs; P=0.0031, Tukey multiple comparison test following one way ANOVA; P=0.0026, F(2,18)=8.456). Remarkably, this was completely rescued by ALCAR treatment (303.3 ± 27.9 μs, P=0.0105 vs 18-month, P=0.9398 vs 1-month; Fig. 2E). As a result of altered synaptic delay, overall synaptic transmission (SD + CD) was significantly slowed down in 18-month old mice (versus 1-month old, P=0.0036 by Tukey multiple comparison test following one-way ANOVA; P=0.0031, F(2,18)=8.087), and was rescued by ALCAR (P=0.0131 vs 18-month, P=0.9555 vs 1-month; Fig. 2F). Because the calyx of Held acts as a sign-inverting relay synapse in the sound localization circuit, these timing errors may contribute to impaired sound localization in older animals, including humans (Brand et al., 2002; Freigang et al., 2015; Grothe et al., 2010).

We examined spontaneous excitatory postsynaptic currents (sEPSC) at the calyx of Held synapse in young and old mice, and in old mice fed ALCAR, to determine if changes in quantal parameters were responsible for increased EPSC size in older mice (Fig. 3). Change in quantal size indicates altered receptor field size, or altered loading of transmitter in synaptic vesicles, while increased frequency may indicate defects in presynaptic calcium buffering, and decreased frequency may indicate a loss of release sites. Frequency of sEPSC events did not change with age or ALCAR treatment (1-month: 6.48 ± 2.73 Hz, N=11; 18-month: 4.75 ± 1.15 Hz, N=6; ALCAR: 4.97 ± 0.92 Hz, N=7; P=0.8331, F(2,21)=0.1842,

One-way ANOVA; Fig. 3A). Similarly, we saw no effect of age or ALCAR treatment on quantal size, estimated as the median sEPSC amplitude (1-month: 69.52 ± 5.89 pA; 18-month: 70.12 ± 11.70 pA; ALCAR: 97.81 ± 14.75 pA; P=0.1147, F(2,21)=2.405, One-way ANOVA; Fig. 3A). Neither age nor ALCAR affected quantal event kinetics, as average decay times for sEPSCs were similar in all conditions (Fig. 3B). Decay time at 1-month was 331.8 ± 24.7 μs, 366.4 ± 25.1 μs at 18 months, and 360.2 ± 40.44 μs following ALCAR treatment (P=0.6706, F(2,22)=0.4069, One-way ANOVA). We conclude that quantal parameters of excitatory glutamatergic transmission at this synapse are not altered during normal aging, or treatment with ALCAR.

3.2.2 Aged synapses show faster and more extensive short-term depression—

As part of the auditory central nervous system, the calyx of Held is a synapse that can reliably respond to several hundred Hertz input frequency, and exhibits short-term presynaptic depression (Gersdorff and Borst, 2002). Therefore, we were interested to see if aging affected short-term plasticity at this synapse. We stimulated the synapse with short trains at 100 Hz (50 pulses), and recorded EPSCs from principal neurons of the MNTB (Figure 4). In synapses from 1-month old mice, depression was monoexponential (decay constant, τ = 35.8 ± 4.1 ms, N=10), and reached a steady-state where synaptic vesicle (SV) release and refilling were balanced (19.12 ± 3.54% of initial EPSC amplitude). In 18-month old mice, depression was slightly faster, but not significantly altered (τ = 24.2 ± 3.2 ms, N=9, P=0.1096 by Tukey multiple comparison test following one-way ANOVA; P=0.0490, F(2,26)=3.393); Fig. 4C) and steady state current was significantly reduced (6.42 ± 1.21%, n=9, P= 0.0108 by Tukey multiple comparison test following one-way ANOVA; P=0.0067, F(2,24)=6.208; Fig. 4D). Surprisingly, this age-related defect in synaptic depression was completely ameliorated in mice that were fed with ALCAR and returned to response kinetics and size indistinguishable from those observed in 1-month old mice (τ = 37.93 ± 5.38 ms, N=8, P= 0.0707 vs 18-month, P=0.9388 vs 1-month; Steady-state = 18.67 ± 3.22%, P= 0.0207 vs 18-month, P = 0.9934 vs 1-month).

Stimulating at higher frequency (300 Hz, 50 pulses) nears the maximum sustainable frequency of this synapse at room temperature. Though substantial monophasic depression was observed (τ = 16.12 ± 2.53 ms, N=11; steady-state = 4.53 ± 1.32% of initial EPSC amplitude), stimulation could be maintained in synapses from 1-month old mice (Figure 5A). In synapses from 18-month old mice, significantly faster and near-complete depression was observed and was often accompanied by frequent failures of EPSCs near the end of the stimulus train (Fig. 5A–B). Depression was significantly faster and more extensive in these older animals (τ = 8.601 ± 1.20 ms, N=11, P=0.0372 by Tukey multiple comparison test following one-way ANOVA; P=0.0146, F(2,27)=4.962; steady-state = 0.52 ± 0.22%, P=0.0252 by Tukey multiple comparison test following one-way ANOVA; P=0.0011, F(2,27)=8.805). Similar to the effect of ALCAR observed at 100 Hz, treatment of 18-month old mice restored transmission akin to that in 1-month old synapses (τ = 17.26 ± 2.57 ms, N=8, P=0.9398 vs 18-month, P= 0.0268 vs 1 Month; steady-state = 0.06898 ± 0.01412, P=0.0010 vs 18-month, P =0.3027 vs 1-month).

3.2.3 Aged synapses have higher SV release probability and slower vesicle refilling rate—Multiple parameters underlying activity-dependent SV dynamics can be inferred using the method of Wesseling and Lo (Wesseling and Lo, 2002), which was recently applied to this synapse for 300 Hz stimulation trains (Mahfooz et al., 2016). This model provides accurate estimations of initial SV release probability (P_r), readily releasable pool (RRP) size, and unitary vesicle refilling rate during a high-frequency train (Figure 5C).

Using this method, SV P_r was estimated to be 0.22 ± 0.02 in 1-month old mice, similar to that previously reported for animals at functional maturity (Chang et al., 2015; Montesinos et al., 2015; Vasileva et al., 2012). In 18-month old mice, P_r was significantly increased relative to 1-month old mice (0.35 ± 0.03, P= 0.0083 by Tukey multiple comparison test following one-way ANOVA; P=0.0004, F(2,26)=10.69). Once again, ALCAR treated mice rescued this phenotype, with P_r similar to 1-month old mice (0.15 ± 0.03, P= 0.0004 vs 18-month, P = 0.3234 vs 1-month; Figure 5C).

Vesicle replenishment of the releasable pool, estimated as a fixed unitary rate during the stimulation train, exhibited a significant decrease in 18-month old mice relative to 1-month old mice (1-month: 3.23 ± 0.24 s^{-1}; 18-month: 1.42 ± 0.22 s^{-1}, P= 0.0003 by Tukey multiple comparison test following one-way ANOVA; P<0.0001, F(2,26)=20.75; Fig. 5C). ALCAR treatment reduced the unitary refilling rate back to levels similar to 1-month old mice (4.11 ± 0.44 s^{-1}, P=0.0001 vs 18-month, P =0.1170 vs 1-month).

One notable characteristic of the calyx of Held synapse is a large RRP distributed across several hundred release sites, and composed of many hundreds to thousands of SVs (Borst and Soria van Hoeve, 2012). We estimated the RRP in 1-month old mice at 1293 ± 140 SVs, within the range of previous reports for slightly younger animals (Guo et al., 2015; Qiu et al., 2015; Schneggenburger et al., 2002). The RRP size was not altered at 18-months (1552 ± 288 SVs) or in response to treatment with ALCAR (1613 ± 319; P=0.6180, F(2,26)=0.4902, One-way ANOVA; Fig. 5C).

Taken together, increased depression and reduced steady-state in older animals appears to stem from two defects: increased initial release probability, and a dramatic decrease in vesicle replenishment rate during ongoing activity. Vesicle replenishment during activity is a calcium and ATP-dependent mechanism (Sakaba and Neher, 2003; 2001a). This mechanistic defect could be fully restored by ALCAR, again suggestive of a mitochondrial etiology.

3.2.4 Recovery of RRP in young and old mice—Given that release-competent vesicle replenishment is impaired during activity in synapses of 18-month old mice, we were interested to determine whether recovery of the RRP was also altered during periods of quiescence between activity bouts. To examine RRP recovery, we used two bouts of 300 Hz stimulation trains, separated by defined rest intervals from 10 ms to 13 sec (Fig. 6A). The recovery curves were adequately fit by a biexponential curve as previously described (Z. Chen et al., 2013). The initial fast recovery phase (τ_{fast}) was slightly slower in 18-month old animals, but was not rescued by ALCAR treatment (1-month: 93.61 ± 23.55 ms, N=9; 18-month: 183.80 ± 21.81 ms, N=10; 18-month ALCAR: 175.3 ± 60.28 ms, N=8, P=0.1443, F(2,24) = 2.101, One-way ANOVA: Fig. 6C). The slower phase of the recovery curve, which

is calcium-independent (Hosoi et al., 2007; Sakaba and Neher, 2001b; Wang and Kaczmarek, 1998), was unaffected in all conditions (1-month: 4.17 ± 0.434 s; 18-month: 3.90 ± 0.38 s; 18-month ALCAR: 3.66 ± 1.22 s; P=0.8876, F(2,24) = 0.1198, One-way ANOVA: Fig. 6D). The balance between fast and slow forms of SV recovery was altered by age, with older mice using a larger proportion of τ_{fast} (1-month: 24.43 ± 1.94 %, 18-month: 36.57 ± 1.86 %, P=0.0486 by Tukey multiple comparison test following one-way ANOVA; P=0.0078, F(2,24)=5.99; Fig. 6C), which was not reversed by administration of ALCAR (41.39 ± 6.086 %, P=0.6051 versus 18-month, P=0.0078 versus 1-month; Fig 6C). Thus, RRP recovery at rest shows a specific increase in the fast component of recovery in older animals, but overall recovery is not affected, or altered by ALCAR treatment.

We could also measure recovery of the first EPSC after RRP depletion, which represents functional recovery of transmission at this synapse. Recovery of the initial EPSC size was faster in older animals, due to an increased contribution of the fast component, through time constants were unaffected (Fig 6E–F). Fast recovery component (τ_{fast}) was 78.37 ± 15.34 at 1-month, 111.6 ± 42.91 at 18-month, and 102.7.7 in ALCAR-treated mice (P=0.7074, F(2,24)=0.3512, one-way ANOVA). Percent τ_{fast} was 16.26 ± 0.88% at 1-month, and increased to 24.69 ± 3.15% at 18-month (P=0.0214 v. 1-month, by Tukey multiple comparison test following one-way ANOVA, P=0.0085, F(2,24)=5.846, one-way ANOVA). In ALCAR mice, the contribution of τ_{fast} was also larger relative to 1-month (25.61 ± 0.62% in ALCAR-treated mice, P=0.0155 v. 1-month). The slow component of recovery for single EPSCs was not affected (5.65 ±0.32 sec at 1-month, 4.86 ±0.94 at 18-month, and 4.51 ± 0.16 in ALCAR-treated mice; P=0.4566, F(2,24)=0.8101, one-way ANOVA; Fig. 6G). This result is similar to what has been shown previously for aged mice in other auditory central synapses (Xie and Manis, 2017). However, recovery of EPSC amplitude was not affected by ALCAR treatment.

4. Discussion

In the present study, we examined age-related changes the efficiency of synaptic transmission at the calyx of Held, from juvenile adults (1-month old) and late middle-age (18- to 21-month old) mice. The calyx of Held synapse has been exploited as a model for understanding excitation secretion coupling in central glutamatergic neurons, and is specialized for high frequency transmission as part of a timing circuit for sound localization in mammals (Baydyuk et al., 2016; Borst and Soria van Hoeve, 2012; Gersdorff and Borst, 2002). Our observations suggest that during aging there is neuronal cell loss in the MNTB, similar to previous reports (Casey and Feldman, 1988; O'Neill et al., 1997). In remaining synapses of the MNTB, we observed severe impairments in transmission timing and SV recycling, resulting in timing errors and increased synaptic depression in the calyx of Held synapse. These defects reduce the efficacy of this synapse to encode temporally sensitive information and is likely to result in diminished sound localization. Treatment of aged mice with the nutritional supplement ALCAR shows improvement in hearing and synaptic plasticity but the mechanism is unknown.

Age-related defects in auditory synaptic transmission

Interestingly, similar age-related defects in transmission and short-term plasticity have been reported at the endbulb of Held, another giant glutamatergic synapse at bushy cell neurons of the cochlear nucleus, which receive efferent input from spiral ganglion cell axons (Xie and Manis, 2017). In this previous study, high frequency stimulation resulted in reduced transmission in older mice and was linked to reduced calcium buffering within the presynaptic terminal, as it could be ameliorated by loading the terminal with EGTA-AM. In contrast, we did not find any apparent defect in calcium buffering, and transmission was not rescued in 18-month old calyx of Held synapses by EGTA-AM (data not shown). Instead, defects in transmission at the calyx of Held seem to be due to impaired synaptic vesicle recycling. These discrepancies suggest that age-related decline in synaptic transmission may be due to multiple mechanisms, and may differ between synapses, even within the same sensory system. A relationship between presbycusis and age-related dementia and cognitive decline has been established, but it is unclear if this link is causal (Deal et al., 2017; Golub, 2017; Wayne and Johnsrude, 2015). Age-related increase in presynaptic short-term depression has been observed in synapses of hippocampus (Landfield and Lynch, 1977). It will be interesting to determine if similar defects in SV recycling are present at forebrain glutamatergic synapses.

ALCAR ameliorates synaptic transmission defects

ALCAR is actively transported across the blood brain barrier, and is necessary for the transport of long-chain fatty acids into the mitochondria for β-oxidation, ATP production, and removal of excess fatty acids (Bieber, 1988). ALCAR treatment has been shown in multiple systems to improve mitochondrial function in CNS, and improve age-related behavioral deficiencies (Aliev et al., 2009; Ando et al., 2001; Hagen et al., 2002; Liu et al., 2002; Mehrotra et al., 2015; Milgram et al., 2007). In addition, ALCAR acts an acute neuroprotectant against ischemic-like loss of transmission in hippocampal slices (Kocsis et al., 2016). ALCAR treatment has been shown previously to not affect multiple parameters of mitochondrial function and behavior in normal young animals (Aliev et al., 2009; Mehrotra et al., 2015) so was not given to juvenile adults used in this study.

Our data clearly illustrate an age-related defect in high-frequency transmission at the calyx of Held synapse, which is rescued by ACLAR treatment. We assume that this defect is due to age-related deterioration of mitochondrial health. But, ALCAR has diverse effects on mitochondrial and cellular function, and an alternative may be that ALCAR is acting to suppress neuroinflammation in older mice. Previous work has established that groups of genes involved in the immune response is a common signature of aging and presbycusis (de Magalhães et al., 2009; Watson et al., 2017). For example, anti-inflammatory treatment with ibuprofen has been shown previously to rescue age-related behavioral impairment (Rogers et al., 2017). ALCAR has been shown to reduce neuroinflammation in aged animals and models of neurodegenerative disease (Afshin-Majd et al., 2017; Karalija et al., 2014; Kazak and Yarim, 2017; Traina, 2016). While it is not clear if the effect of ALCAR is due to improved glial or neuronal health, it is parsimonious to assume that increased mitochondrial function in the presynaptic terminal acts to enhance activity-dependent SV recycling.

5. Conclusions

Aging results in increased expression of immune-response genes in the CNS, and reduced mitochodnrial function. Synaptic transmission timing is defective in aged mice at the calyx of Held, and these errors are likely to have significant contribution to loss of function in the sound localization circuit. Specifically, older mice lose temporal fidelity at the calyx synapse, which would be predicted to result in binaural timing errors. Short-term plasticity is also impaired, resulting in substantially decreased transmission, and impairing circuit function. In older mice, recovery from depletion of synaptic vesicles in the readily releasable pool is faster than in juvenile adults.

Remarkably, treatment with ALCAR restores transmission defects in timing and short-term plasticity, while not affecting recovery from depression. The functional defect of this circuit mirrors age-related transmission changes in other regions of the CNS, and it is likely that mechanisms underlying functional recovery following ALCAR treatment are also shared. Future work should address the downstream targets of ALCAR treatment at the presynaptic terminal, and whether treatment is accompanied by restoration of youthful signature of gene expression in the brain, and in particular in relation to mitochondrial function and immune response.

Supplementary Material

Refer to Web version on PubMed Central for supplementary material.

Acknowledgments

Funding: This work was supported by The National Institutes of Health (GM110767, GM103554, GM103650, GM103440). The funding source had no involvement in the study design, collection, analysis or interpretation of the data, or writing and submission of this report.

Abbreviations

SOC	superior olivary complex
MNTB	medial nucleus of the trapezoid body
ALCAR	Acetyl-l-carnitine hydrochloride
EPSC	excitatory postsynaptic current

References

Afshin-Majd S, Bashiri K, Kiasalari Z, Baluchnejadmojarad T, Sedaghat R, Roghani M. Acetyl-l-carnitine protects dopaminergic nigrostriatal pathway in 6-hydroxydopamine-induced model of Parkinson’s disease in the rat. Biomed Pharmacother. 2017; 89:1–9. DOI: 10.1016/j.biopha.2017.02.007 [PubMed: 28199883]

Aliev G, Liu J, Shenk JC, Fischbach K, Pacheco GJ, Chen SG, Obrenovich ME, Ward WF, Richardson AG, Smith MA, Gasimov E, Perry G, Ames BN. Neuronal mitochondrial amelioration by feeding acetyl-L-carnitine and lipoic acid to aged rats. J Cell Mol Med. 2009; 13:320–333. DOI: 10.1111/j.1582-4934.2008.00324.x [PubMed: 18373733]

Ando S, Tadenuma T, Tanaka Y, Fukui F, Kobayashi S, Ohashi Y, Kawabata T. Enhancement of learning capacity and cholinergic synaptic function by carnitine in aging rats. J Neurosci Res. 2001; 66:266–271. DOI: 10.1002/jnr.1220 [PubMed: 11592123]

Barnes CA, Markowska AL, Ingram DK, Kametani H, Spangler EL, Lemken VJ, Olton DS. Acetyl-1-carnitine. 2: Effects on learning and memory performance of aged rats in simple and complex mazes. Neurobiol Aging. 1990; 11:499–506. DOI: 10.1016/0197-4580(90)90110-L [PubMed: 2234280]

Baydyuk M, Xu J, Wu LGG. The calyx of Held in the auditory system: Structure, function, and development. Hearing Research. 2016; 338:22–31. DOI: 10.1016/j.heares.2016.03.009 [PubMed: 27018297]

Bieber LL. Carnitine. Annu Rev Biochem. 1988; 57:261–283. DOI: 10.1146/annurev.bi.57.070188.001401 [PubMed: 3052273]

Borst JGG, Soria van Hoeve JSS. The calyx of held synapse: from model synapse to auditory relay. Annu Rev Physiol. 2012; 74:199–224. DOI: 10.1146/annurev-physiol-020911-153236 [PubMed: 22035348]

Brand A, Behrend O, Marquardt T, McAlpine D, Grothe B. Precise inhibition is essential for microsecond interaural time difference coding. Nature. 2002; 417:543–547. DOI: 10.1038/417543a [PubMed: 12037566]

Cant NB, Benson CG. Parallel auditory pathways: projection patterns of the different neuronal populations in the dorsal and ventral cochlear nuclei. Brain Research Bulletin. 2003; 60:457–474. DOI: 10.1016/S0361-9230(03)00050-9 [PubMed: 12787867]

Casey MA, Feldman ML. Age-related loss of synaptic terminals in the rat medial nucleus of the trapezoid body. NSC. 1988; 24:189–194. DOI: 10.1016/0306-4522(88)90322-3

Chang S, Reim K, Pedersen M, Neher E, Brose N, Taschenberger H. Complexin stabilizes newly primed synaptic vesicles and prevents their premature fusion at the mouse calyx of held synapse. Journal of Neuroscience. 2015; 35:8272–8290. DOI: 10.1523/JNEUROSCI.4841-14.2015 [PubMed: 26019341]

Chen L, Na R, Ran Q. Enhanced defense against mitochondrial hydrogen peroxide attenuates age-associated cognition decline. Neurobiol Aging. 2014; 35:2552–2561. DOI: 10.1016/j.neurobiolaging.2014.05.007 [PubMed: 24906890]

Chen Z, Cooper B, Kalla S, Varoqueaux F, Young SM Jr. The Munc13 proteins differentially regulate readily releasable pool dynamics and calcium-dependent recovery at a central synapse. Journal of Neuroscience. 2013; 33:8336–8351. DOI: 10.1523/JNEUROSCI.5128-12.2013 [PubMed: 23658173]

Choi SH, Choi CH. Noise-Induced Neural Degeneration and Therapeutic Effect of Antioxidant Drugs. J Audiol Otol. 2015; 19:111–119. DOI: 10.7874/jao.2015.19.3.111 [PubMed: 26771008]

Coleman JKM, Kopke RD, Liu J, Ge X, Harper EA, Jones GE, Cater TL, Jackson RL. Pharmacological rescue of noise induced hearing loss using N-acetylcysteine and acetyl-l-carnitine. Hearing Research. 2007; 226:104–113. DOI: 10.1016/j.heares.2006.08.008 [PubMed: 17023129]

de Magalhães JP, Curado J, Church GM. Meta-analysis of age-related gene expression profiles identifies common signatures of aging. Bioinformatics. 2009; 25:875–881. DOI: 10.1093/bioinformatics/btp073 [PubMed: 19189975]

Deal JA, Betz J, Yaffe K, Harris T, Purchase-Helzner E, Satterfield S, Pratt S, Govil N, Simonsick EM, Lin FR. Health ABC Study Group. Hearing Impairment and Incident Dementia and Cognitive Decline in Older Adults: The Health ABC Study. J Gerontol A Biol Sci Med Sci. 2017; 72:703–709. DOI: 10.1093/gerona/glw069 [PubMed: 27071780]

Dondzillo A, Sätzler K, Horstmann H, Altrock WD, Gundelfinger ED, Kuner T. Targeted three-dimensional immunohistochemistry reveals localization of presynaptic proteins Bassoon and Piccolo in the rat calyx of Held before and after the onset of hearing. J Comp Neurol. 2010; 518:1008–1029. DOI: 10.1002/cne.22260 [PubMed: 20127803]

Eggermont JJ. Acquired hearing loss and brain plasticity. Hearing Research. 2017; 343:176–190. DOI: 10.1016/j.heares.2016.05.008 [PubMed: 27233916]

Fedchyshyn MJ, Wang LYY. Activity-dependent changes in temporal components of neurotransmission at the juvenile mouse calyx of Held synapse. The Journal of Physiology. 2007; 581:581–602. DOI: 10.1113/jphysiol.2007.129833 [PubMed: 17347264]

Freigang C, Richter N, Rübsamen R, Ludwig AA. Age-related changes in sound localisation ability. Cell Tissue Res. 2015; 361:371–386. DOI: 10.1007/s00441-015-2230-8 [PubMed: 26077928]

Gates GA, Mills JH. Presbycusis. Lancet. 2005; 366:1111–1120. DOI: 10.1016/S0140-6736(05)67423-5 [PubMed: 16182900]

von Gersdorff H, Borst JGG. Short-term plasticity at the calyx of held. Nat Rev Neurosci. 2002; 3:53–64. DOI: 10.1038/nrn705 [PubMed: 11823805]

Golub JS. Brain changes associated with age-related hearing loss. Curr Opin Otolaryngol Head Neck Surg. 2017; 25:347–352. DOI: 10.1097/MOO.0000000000000387 [PubMed: 28661962]

Grothe B, Pecka M, McAlpine D. Mechanisms of sound localization in mammals. Physiol Rev. 2010; 90:983–1012. DOI: 10.1152/physrev.00026.2009 [PubMed: 20664077]

Guo J, Ge JL, Hao M, Sun ZC, Wu XS, Zhu JB, Wang W, Yao PT, Lin W, Xue L. A three-pool model dissecting readily releasable pool replenishment at the calyx of held. Sci Rep. 2015; 5:9517.doi: 10.1038/srep09517 [PubMed: 25825223]

Hagen TM, Liu J, Lykkesfeldt J, Wehr CM, Ingersoll RT, Vinarsky V, Bartholomew JC, Ames BN. Feeding acetyl-L-carnitine and lipoic acid to old rats significantly improves metabolic function while decreasing oxidative stress. Proc Natl Acad Sci USA. 2002; 99:1870–1875. DOI: 10.1073/pnas.261708898 [PubMed: 11854487]

Han C, Someya S. Mouse models of age-related mitochondrial neurosensory hearing loss. Molecular and Cellular Neuroscience. 2013; 55:95–100. DOI: 10.1016/j.mcn.2012.07.004 [PubMed: 22820179]

Harrison JM, Warr WB. A study of the cochlear nuclei and ascending auditory pathways of the medulla. J Comp Neurol. 1962; 119:341–379. [PubMed: 13952992]

Hawley ML, Litovsky RY, Culling JF. The benefit of binaural hearing in a cocktail party: effect of location and type of interferer. J Acoust Soc Am. 2004; 115:833–843. [PubMed: 15000195]

Heffner, HE., Heffner, RS., Koay, G. Handbook of Mouse Auditory Research. In: Willott, JF., editor. From Behavior to Molecular Biology. CRC Press; 2001. p. 31-35.

Hosoi N, Sakaba T, Neher E. Quantitative analysis of calcium-dependent vesicle recruitment and its functional role at the calyx of Held synapse. Journal of Neuroscience. 2007; 27:14286–14298. DOI: 10.1523/JNEUROSCI.4122-07.2007 [PubMed: 18160636]

Huang Q, Aluise CD, Joshi G, Sultana R, St Clair DK, Markesbery WR, Butterfield DA. Potential in vivo amelioration by N-acetyl-L-cysteine of oxidative stress in brain in human double mutant APP/PS-1 knock-in mice: toward therapeutic modulation of mild cognitive impairment. J Neurosci Res. 2010; 88:2618–2629. DOI: 10.1002/jnr.22422 [PubMed: 20648652]

Humes LE, Dubno JR, Gordon-Salant S, Lister JJ, Cacace AT, Cruickshanks KJ, Gates GA, Wilson RH, Wingfield A. Central presbycusis: a review and evaluation of the evidence. J Am Acad Audiol. 2012; 23:635–666. DOI: 10.3766/jaaa.23.8.5 [PubMed: 22967738]

Hunter KP, Willott JF. Aging and the auditory brainstem response in mice with severe or minimal presbycusis. Hearing Research. 1987; 30:207–218. DOI: 10.1016/0378-5955(87)90137-7 [PubMed: 3680066]

Karalija A, Novikova LN, Kingham PJ, Wiberg M, Novikov LN. The effects of N-acetyl-cysteine and acetyl-l-carnitine on neural survival, neuroinflammation and regeneration following spinal cord injury. Neuroscience. 2014; 269:143–151. DOI: 10.1016/j.neuroscience.2014.03.042 [PubMed: 24680856]

Kazak F, Yarim GF. Neuroprotective effects of acetyl-l-carnitine on lipopolysaccharide-induced neuroinflammation in mice: Involvement of brain-derived neurotrophic factor. Neuroscience Letters. 2017; 658:32–36. DOI: 10.1016/j.neulet.2017.07.059 [PubMed: 28822835]

Keithley EM, Canto C, Zheng QY, Fischel-Ghodsian N, Johnson KR. Age-related hearing loss and the ahl locus in mice. Hearing Research. 2004; 188:21–28. DOI: 10.1016/S0378-5955(03)00365-4 [PubMed: 14759567]

Kocsis K, Frank R, Szabó J, Knapp L, Kis Z, Farkas T, Vécsei L, Toldi J. Acetyl-l-carnitine restores synaptic transmission and enhances the inducibility of stable LTP after oxygen-glucose

deprivation. Neuroscience. 2016; 332:203–211. DOI: 10.1016/j.neuroscience.2016.06.046 [PubMed: 27378558]

Kopke R, Bielefeld E, Liu J, Zheng J, Jackson R, Henderson D, Coleman JKM. Prevention of impulse noise-induced hearing loss with antioxidants. Acta Otolaryngol. 2005; 125:235–243. [PubMed: 15966690]

Landfield PW, Lynch G. Impaired monosynaptic potentiation in in vitro hippocampal slices from aged, memory-deficient rats. J Gerontol. 1977; 32:523–533. [PubMed: 196001]

Lin MT, Beal MF. Mitochondrial dysfunction and oxidative stress in neurodegenerative diseases. Nature. 2006; 443:787–795. DOI: 10.1038/nature05292 [PubMed: 17051205]

Liu J, Head E, Gharib AM, Yuan W, Ingersoll RT, Hagen TM, Cotman CW, Ames BN. Memory loss in old rats is associated with brain mitochondrial decay and RNA/DNA oxidation: partial reversal by feeding acetyl-L-carnitine and/or R-alpha -lipoic acid. Proc Natl Acad Sci USA. 2002; 99:2356–2361. DOI: 10.1073/pnas.261709299 [PubMed: 11854529]

Lujan B, Kushmerick C, Banerjee TD, Dagda RK, Renden R. Glycolysis selectively shapes the presynaptic action potential waveform. J Neurophysiol. 2016; 116:2523–2540. DOI: 10.1152/jn.00629.2016 [PubMed: 27605535]

Mahfooz K, Singh M, Renden R, Wesseling JF. A Well-Defined Readily Releasable Pool with Fixed Capacity for Storing Vesicles at Calyx of Held. PLoS Computational Biology. 2016; 12:e1004855.doi: 10.1371/journal.pcbi.1004855 [PubMed: 27035349]

Mehrotra A, Kanwal A, Banerjee SK, Sandhir R. Mitochondrial modulators in experimental Huntington's disease: reversal of mitochondrial dysfunctions and cognitive deficits. Neurobiol Aging. 2015; 36:2186–2200. DOI: 10.1016/j.neurobiolaging.2015.02.004 [PubMed: 25976011]

Milgram NW, Araujo JA, Hagen TM, Treadwell BV, Ames BN. Acetyl-L-carnitine and alpha-lipoic acid supplementation of aged beagle dogs improves learning in two landmark discrimination tests. FASEB J. 2007; 21:3756–3762. DOI: 10.1096/fj.07-8531com [PubMed: 17622567]

Montesinos MS, Dong W, Goff K, Das B, Guerrero-Given D, Schmalzigaug R, Premont RT, Satterfield R, Kamasawa N, Young SM Jr. Presynaptic Deletion of GIT Proteins Results in Increased Synaptic Strength at a Mammalian Central Synapse. Neuron. 2015; 88:918–925. DOI: 10.1016/j.neuron.2015.10.042 [PubMed: 26637799]

O'Neill WE, Zettel ML, Whittemore KR, Frisina RD. Calbindin D-28k immunoreactivity in the medial nucleus of the trapezoid body declines with age in C57BL/6, but not CBA/CaJ, mice. Hearing Research. 1997; 112:158–166. DOI: 10.1016/S0378-5955(97)00116-0 [PubMed: 9367238]

Qiu X, Zhu Q, Sun JY. Quantitative analysis of vesicle recycling at the calyx of Held synapse. Proceedings of the National Academy of Sciences. 2015; 112:4779–4784. DOI: 10.1073/pnas.1424597112

Rogers JT, Liu CC, Zhao N, Wang J, Putzke T, Yang L, Shinohara M, Fryer JD, Kanekiyo T, Bu G. Subacute ibuprofen treatment rescues the synaptic and cognitive deficits in advanced-aged mice. Neurobiol Aging. 2017; 53:112–121. DOI: 10.1016/j.neurobiolaging.2017.02.001 [PubMed: 28254590]

Sakaba T, Neher E. Involvement of actin polymerization in vesicle recruitment at the calyx of Held synapse. Journal of Neuroscience. 2003; 23:837–846. [PubMed: 12574412]

Sakaba T, Neher E. Quantitative relationship between transmitter release and calcium current at the calyx of held synapse. J Neurosci. 2001a; 21:462–476. [PubMed: 11160426]

Sakaba T, Neher E. Calmodulin mediates rapid recruitment of fast-releasing synaptic vesicles at a calyx-type synapse. Neuron. 2001b; 32:1119–1131. [PubMed: 11754842]

Schneggenburger R, Sakaba T, Neher E. Vesicle pools and short-term synaptic depression: lessons from a large synapse. Trends Neurosci. 2002; 25:206–212. [PubMed: 11998689]

Someya S, Prolla TA. Mitochondrial oxidative damage and apoptosis in age-related hearing loss. Mech Ageing Dev. 2010; 131:480–486. DOI: 10.1016/j.mad.2010.04.006 [PubMed: 20434479]

Takami C, Eguchi K, Hori T, Takahashi T. Impact of vesicular glutamate leakage on synaptic transmission at the calyx of Held. The Journal of Physiology. 2017; 595:1263–1271. DOI: 10.1113/JP273467 [PubMed: 27801501]

Traina G. The neurobiology of acetyl-L-carnitine. Front Biosci (Landmark Ed). 2016; 21:1314–1329. [PubMed: 27100509]

Vasileva M, Horstmann H, Geumann C, Gitler D, Kuner T. Synapsin-dependent reserve pool of synaptic vesicles supports replenishment of the readily releasable pool under intense synaptic transmission. European Journal of Neuroscience. 2012; 36:3005–3020. DOI: 10.1111/j.1460-9568.2012.08225.x [PubMed: 22805168]

Wang LYY, Kaczmarek LK. High-frequency firing helps replenish the readily releasable pool of synaptic vesicles. Nature. 1998; 394:384–388. DOI: 10.1038/28645 [PubMed: 9690475]

Watson N, Ding B, Zhu X, Frisina RD. Chronic inflammation - inflammaging - in the ageing cochlea: A novel target for future presbycusis therapy. Ageing Res Rev. 2017; 40:142–148. DOI: 10.1016/j.arr.2017.10.002 [PubMed: 29017893]

Wayne RV, Johnsrude IS. A review of causal mechanisms underlying the link between age-related hearing loss and cognitive decline. Ageing Research Reviews. 2015; 23:154–166. DOI: 10.1016/j.arr.2015.06.002 [PubMed: 26123097]

Wesseling JF, Lo DC. Limit on the role of activity in controlling the release-ready supply of synaptic vesicles. J Neurosci. 2002; 22:9708–9720. DOI: 10.1126/science.275.5297.221 [PubMed: 12427826]

Willott JF, Parham K, Hunter KP. Comparison of the auditory sensitivity of neurons in the cochlear nucleus and inferior colliculus of young and aging C57BL/6J and CBA/J mice. Hearing Research. 1991; 53:78–94. DOI: 10.1016/0378-5955(91)90215-U [PubMed: 2066290]

Wolak T, Cieśla K, Lorens A, Kochanek K, Lewandowska M, Rusiniak M, Pluta A, Wójcik J, Skarżyński H. Tonotopic organisation of the auditory cortex in sloping sensorineural hearing loss. Hearing Research. 2017; 355:81–96. DOI: 10.1016/j.heares.2017.09.012 [PubMed: 28987787]

Wong AYC, Graham BP, Billups B, Forsythe ID. Distinguishing between presynaptic and postsynaptic mechanisms of short-term depression during action potential trains. Journal of Neuroscience. 2003; 23:4868–4877. [PubMed: 12832509]

Xie R. Transmission of auditory sensory information decreases in rate and temporal precision at the endbulb of Held synapse during age-related hearing loss. J Neurophysiol. 2016; 116:2695–2705. DOI: 10.1152/jn.00472.2016 [PubMed: 27683884]

Xie R, Manis PB. Synaptic transmission at the endbulb of Held deteriorates during age-related hearing loss. The Journal of Physiology. 2017; 595:919–934. DOI: 10.1113/JP272683 [PubMed: 27618790]

Xie R, Manis PB. Glycinergic synaptic transmission in the cochlear nucleus of mice with normal hearing and age-related hearing loss. J Neurophysiol. 2013; 110:1848–1859. DOI: 10.1152/jn.00151.2013 [PubMed: 23904491]

- Electrophysiology recordings from the calyx of Held show increased short-term depression in aged (18–21 month old) mice.
- Synaptic timing at the calyx of Held is also defective in aged mice.
- Both synaptic defects could be fully reversed by acetyl-l-carnitine.

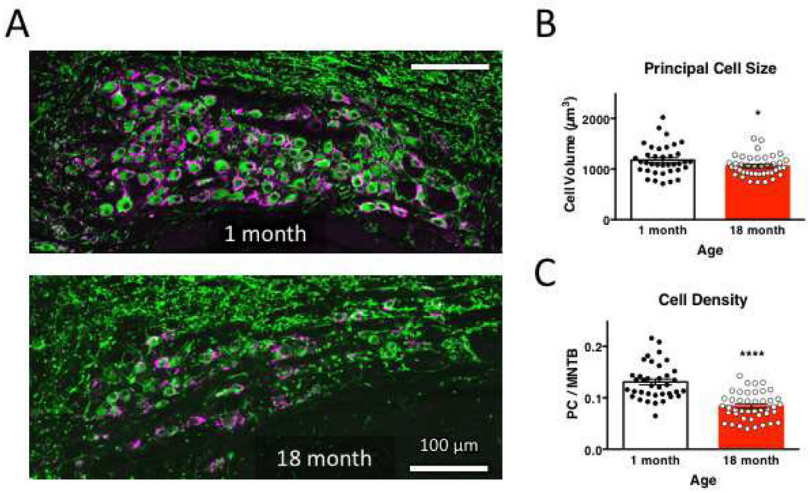

Figure 1. MNTB neuron size and density is attenuated with age

A. Neurons in fixed coronal slices from 1-month (top) and 18-month old mice (bottom) were identified by anti-MAP2 immunoreactivity, and the presynaptic calyceal terminal stained with vGluT1. Images have shared orientation, with midline to the right, dorsal up. Scale bar is 100 µm in both images. **B.** Neuronal cell size was evaluated as volume of MAP2-positive signal in 9–15 µm thick confocal stacks, and is significantly reduced at 18 months, relative to neurons in 1-month old MNTB. **C.** Neuronal cell density was evaluated as the area occupied by MAP2-positive signal within the MNTB nucleus, and was substantially reduced in older mice.

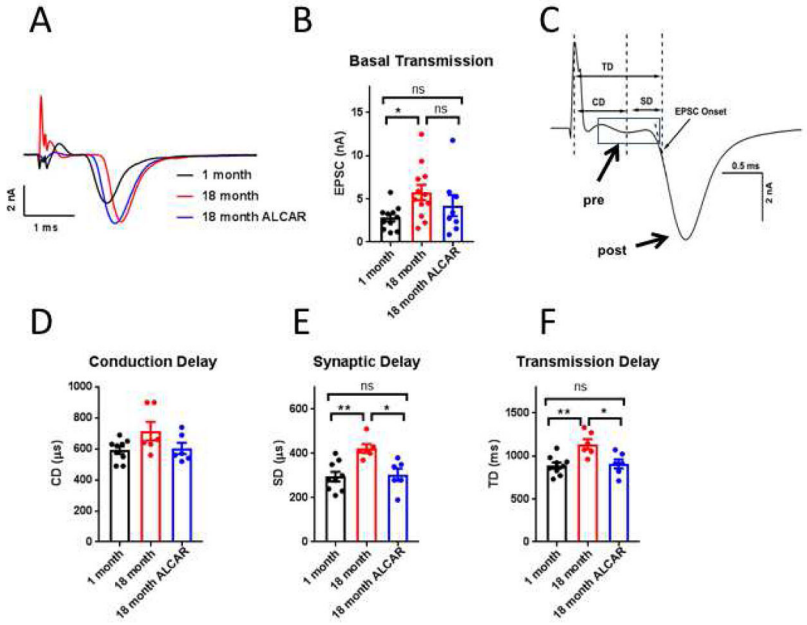

Figure 2. Basal Synaptic transmission is severely affected in old mice, and can be improved by ALCAR

A. Representative traces showing evoked EPSCs from 1 month (black), 18 month (red) and 18 month ALCAR-treated mice (blue). Several (10–20) traces were averaged per cell. **B.** Summary plot showing evoked response amplitudes. **C.** The temporal components of synaptic transmission are defined as in Fedchyshyn & Wang 2007, and were calculated using the maximum curvature method. **D.** Summary plot of conduction delay in 1-month and 18-month mice, and 18-month mice treated with ALCAR. **E.** Summary plot of synaptic delay shows an age-related increase, which is rescued with ALCAR. **F.** Summary plot of transmission delays (CD + SD) show increased delay in older mice, which is reversed by ALCAR.

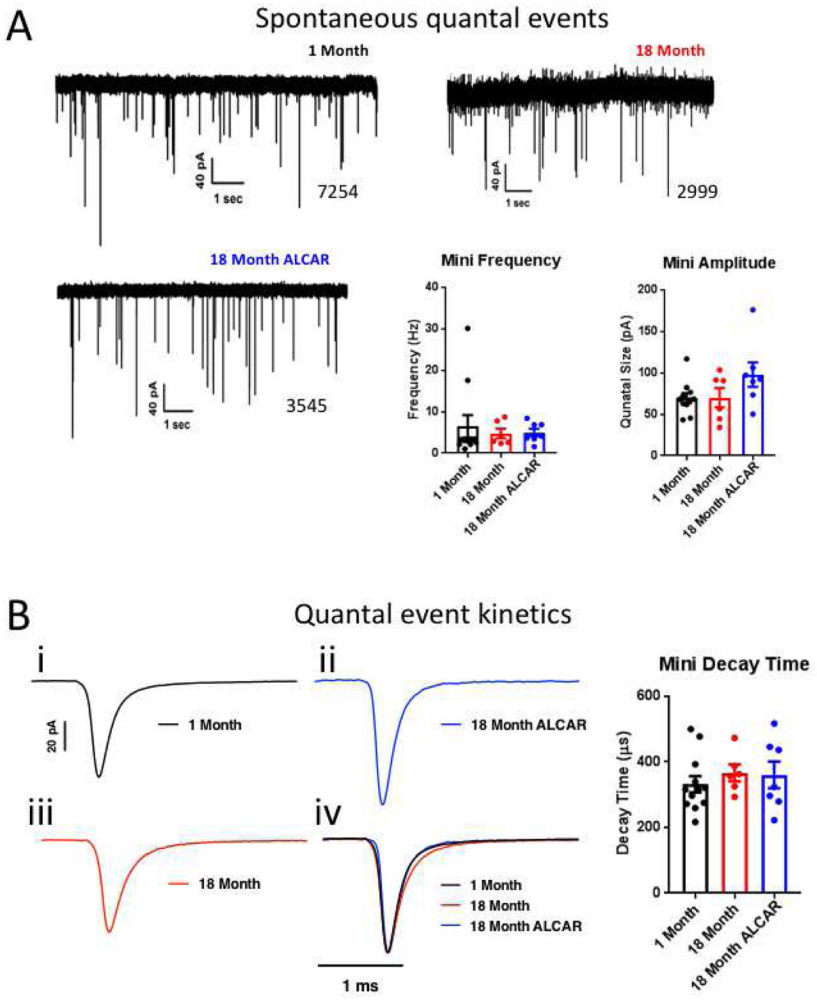

Figure 3. Spontaneous activity does not change with age

A. example traces of spontaneous activity in juvenile adult and aged mice, and aged mice after one month treatment with ALCAR. Summary data show that spontaneous activity is not affected by age or ALCAR treatment, and quantal size is not altered. **B.** Neither age nor ALCAR affected quantal event kinetics, as average decay times for sEPSCs were similar in all conditions. Example traces are averaged for 1500 events per condition. Scale bars are shared between traces i–iv. Traces are normalized to peak in iv.

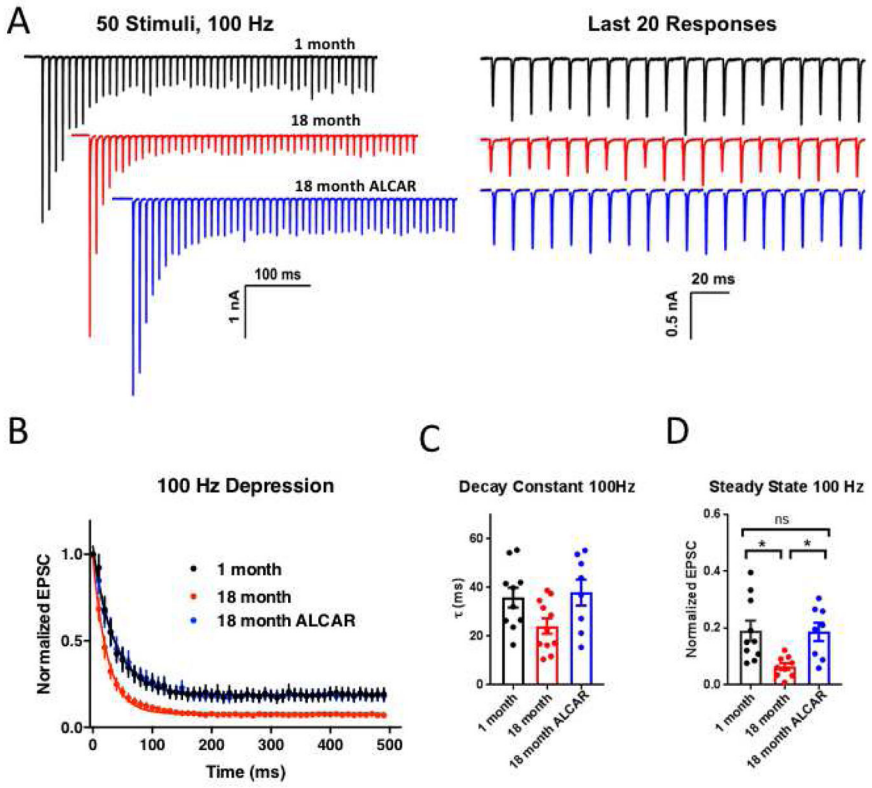

Figure 4. Short-term depression is profoundly increased in older mice

A. Example traces of responses to 100 Hz stimulation, illustrating greater short-term depression in synapses from older mice (18-month, red traces). **B.** Summary plot of EPSC amplitude during the stimulus train, normalized to the amplitude of the first response. **C.** Summary plot of decay constant derived from monoexponential fit of depression curves per cell, as shown in B. **D.** Summary plot of steady-state evoked amplitudes obtained per cell from trains between 300–500 ms.

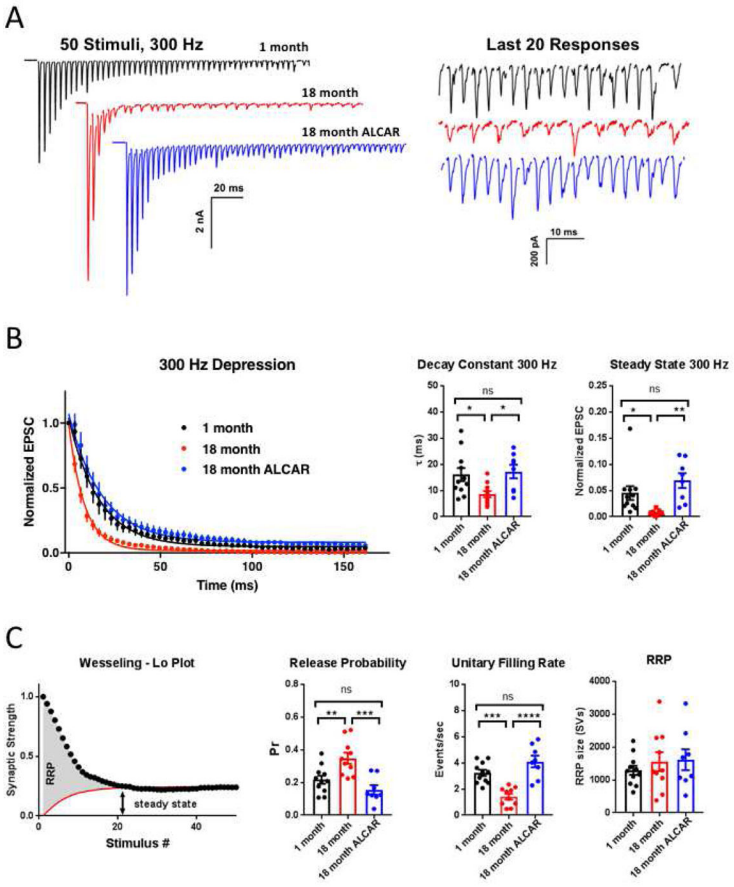

Figure 5. High-frequency stimulation at 300 Hz reveals defects in refilling kinetics underlie enhanced depression

A. Representative traces showing responses to 300 Hz stimulus train. Left panel shows expanded traces near the end of the stimulus train, illustrating transmission failures in synapses from 18-month old mice (red). **B.** Summary plot of EPSC amplitude during the train, normalized to the amplitude of the first response. Summary plot of the paired pulse ratio, decay constant and steady-state, per cell, from monoexponential fit to decay curves. Steady-state was measured as average response near the end of the train, between 133–165 ms. **C.** Illustration of exponential fit method for estimating RRP size, as per Wesseling and Lo, 2002. A constant unitary refilling rate was used to estimate refilling. Summary data of release probability, unitary refilling rate, and readily-releasable pool estimates were generated per cell.

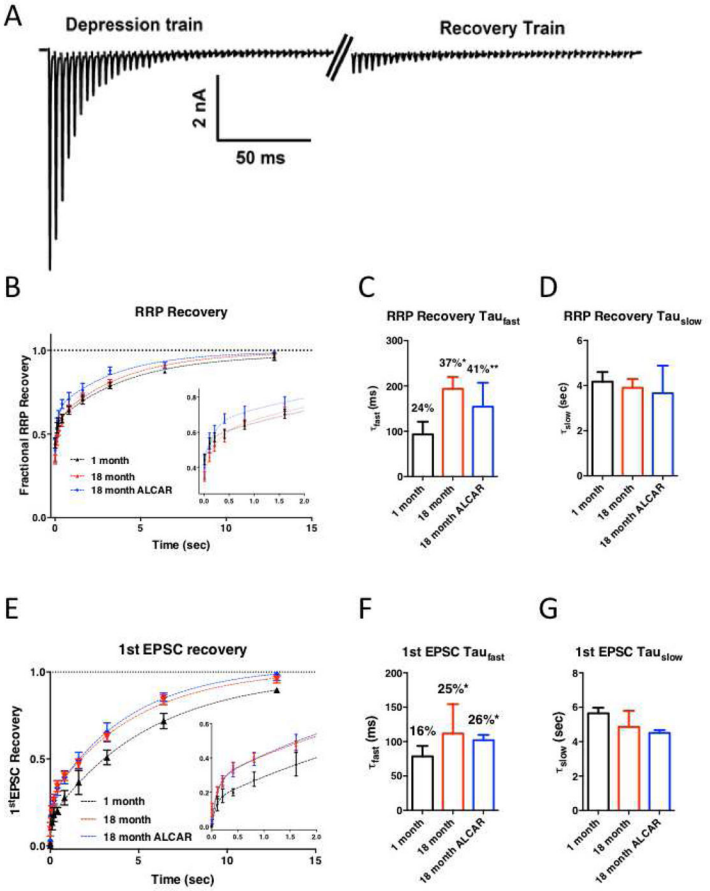

Figure 6. Readily-releasable pool recovery at rest is impaired in older mice, and is not rescued by ALCAR

A. Example trace illustrating the recovery from depression protocol. The synapse was stimulated with a 150 ms train at 300 Hz to deplete the RRP, followed by recovery periods ranging from 10 ms to 12 sec before a second bout of the stimulus train. RRP recovery was estimated by comparing the charge integral between the two trains, after subtracting stimulus artifacts. **B.** Summary of RRP recovery. Recovery curves were adequately fit with a biexponential. Inset shows early phase of recovery. **C.** Summary plot of the fast time constants for recovery, as well as the percentage of contribution of the fast component to recovery. Asterisks illustrate significant increase compared to synapses in 1-month old animals. **D.** Summary plot for slow component of recovery. **E**. Summary of recovery of single EPSC following depression. Recovery could be adequately described by a biexponential. Inset shows the early phase of recovery on an expanded scale. **F**. Summary plot of the fast time constants for recovery, as well as the percentage of contribution of the fast component to recovery. Asterisks illustrate significant increase compared to synapses in 1-month old animals. **G**. Summary plot for slow component of recovery.